



HAL
open science

Sensorless control of a DC series motor

Leonardo Amet, Malek Ghanes, Jean-Pierre Barbot

► **To cite this version:**

Leonardo Amet, Malek Ghanes, Jean-Pierre Barbot. Sensorless control of a DC series motor. IFAC ALCOSP, Jul 2013, Caen, France. hal-00923720

HAL Id: hal-00923720

<https://inria.hal.science/hal-00923720>

Submitted on 4 Jan 2014

HAL is a multi-disciplinary open access archive for the deposit and dissemination of scientific research documents, whether they are published or not. The documents may come from teaching and research institutions in France or abroad, or from public or private research centers.

L'archive ouverte pluridisciplinaire **HAL**, est destinée au dépôt et à la diffusion de documents scientifiques de niveau recherche, publiés ou non, émanant des établissements d'enseignement et de recherche français ou étrangers, des laboratoires publics ou privés.

Super Twisting based step-by-step observer for a DC series motor

Leonardo J. Amet^{*,**} Malek Ghanes^{**} Jean-Pierre Barbot^{**}

** GS Maintenance
16, rue Henri Schneider
77430, Champagne sur Seine, France
leonardo.amet@ensea.fr*

*** ECS - Lab, ENSEA
6, Avenue du Ponceau
95014, Cergy-Pontoise cedex, France.
ghanes@ensea.fr, barbot@ensea.fr*

Abstract: In this paper, a super twisting based step-by-step observer for a DC series motor is proposed. In this context, an observability analysis is performed, revealing an observability singularity at zero current. In order to overcome this problem we propose the joint use of an estimator and an observer. The entire system is validated, by means of simulations, in the context of a sensorless speed control.

1. INTRODUCTION

Among the electrical machines used in industry, the DC motor is one of the simplest because it is governed by continuous voltages and currents. In addition, it presents a great flexibility since it can be configured in several different ways, depending on the connection between stator and armature windings. These configurations present different characteristics, allowing the machine to be adapted to the constraints of its specific application.

In this work, we consider the *DC series motor*, in which the field circuit is connected in series with the armature circuit. Two advantages arise from this electrical connection: on the one hand, only one static converter (e.g. controlled rectifier) is needed; on the other hand, the electromagnetic torque produced is proportional to the square of the current (under linear electromagnetic flux conditions). For this reason, DC series motors are used in applications where high starting torques are needed, such as trains, elevators, hoists; or to produce high torque at slow speeds in applications such as dragline excavation or oil drilling.

The mathematical model of the DC series motor is nonlinear, which inspired the application of different control techniques, ranging from open loop to nonlinear techniques. In Santana et al. [2002] and [Siller-Alcalá et al., 2011] two open-loop strategies are presented, based on PWM and nonlinear predictive techniques, respectively; in the context of closed-loop control strategies we found techniques such as fuzzy tuned PI controllers (Iracleous and Alexandridis [1995a]), singular perturbation approach (Iracleous and Alexandridis [1995b]), feedback linearization design (Chiasson [1994], Mehta and Chiasson [1998]), backstepping method (Burridge and Qu [2003], Dongbo [2008]) and the application of port-controlled Hamiltonian systems equivalence (Iracleous [2009]).

In order to implement closed-loop control techniques, the speed is usually measured by means of mechanical sensors,

which implies higher economical costs and increases the complexity of the system. In addition, in some applications, mechanical components are subject to very harsh conditions, in which the speed sensor is susceptible to failure. These reasons leads us to consider replacing them with some speed estimation technique.

DC series motors present an observability singularity at zero current, so special attention must be paid when estimating the speed near this condition. In Boizot et al. [2007a], Boizot et al. [2007b] and Boizot [2010], the authors propose the application of Adaptive Extended and High-Gain Extended Kalman filters in the observable zone, and compare their performances with those of the Extended Kalman Filter; nevertheless, no solution is given to deal with the observability singularity and no sensorless control is implemented. In Chiasson [1994] and Mehta and Chiasson [1998], a nonlinear observer (with linear error dynamics) is presented, showing that sensorless control of the DC machine is feasible. However, no approach is provided to deal with the observer singularity.

In this work, we present preliminary results of a speed sensorless control for the DC series machine. Firstly, a mathematical model is developed in section 2. In section 3 an observability analysis is performed, revealing an observability singularity at zero current. In the observable zone, a *step-by-step* observer (Floquet and Barbot [2007]) based on *second order sliding modes differentiators* (Levant [1998]) is designed in section 4, taking advantage of its good properties such as finite time convergence, robustness, and design simplicity with respect to noise (see Angulo et al. [2012]). Near the observability singularity, we propose a simple estimator in section 5, which allows the system to work properly near zero current. In section 6 we validate the association observer/estimator in the context of a sensorless speed control, based on classical proportional-integral (PI) techniques, by means of com-

puter simulations. At last, we present the conclusion and perspectives in section 7.

2. MATHEMATICAL MODEL

In the DC series motor, the field and armature windings are connected in series. The dynamics of the current of this circuit is given by:

$$\frac{d(L_a i + \phi_f(i))}{dt} = -(R_f + R_a) i - e + v \quad (1)$$

with $e = K_m \phi_f(i) \omega$, where:

- L_a is the inductance of the armature winding,
- $\phi_f(i)$ is the flux created by the field circuit,
- R_f and R_a are the field and armature circuit resistances, respectively,
- e is the back electromotive force (back EMF)
- K_m is the back EMF constant,
- ω is the angular speed in rad/s ,
- v is the voltage applied to the machine.

In this work, the flux $\phi(i)$ is considered to be linear, hence, it can be modeled as follows:

$$\phi_f(i) = L_f i \quad (2)$$

where L_f is the inductance of the field circuit. Under this assumption, equation (1) can be rewritten as follows:

$$L \frac{di}{dt} = -R i - K_m L_f i \omega + v \quad (3)$$

with $R = R_a + R_f$ and $L = L_a + L_f$.

On the other hand, we have the mechanical subsystem, whose dynamics is given by:

$$J \frac{d\omega}{dt} = \Gamma_{em} - B \omega - \Gamma_L \quad (4)$$

where

- J is the moment of inertia,
- B is the viscous friction,
- Γ_{em} is the electromagnetic torque developed by the machine and
- Γ_L is the load torque.

The electromagnetic torque is given by the following equation:

$$\Gamma_{em} = K \phi(i) i \quad (5)$$

where K is the torque constant. Under the assumption of ideal electromechanical energy conversion, and considering linear flux (equation (2)) we can write:

$$\begin{aligned} e i &= \Gamma_{em} \omega \\ K_m L_f i^2 \omega &= K L_f i^2 \omega \end{aligned} \quad (6)$$

hence

$$K = K_m \quad (7)$$

Replacing (5) to (7) in (4) gives:

$$J \frac{d\omega}{dt} = \Gamma_{em} - B \omega - \Gamma_L \quad (8)$$

The model of the DC series motor is obtained rewriting (3) and (8) as follows:

$$\begin{cases} \frac{di}{dt} = \frac{1}{L} (-Ri - K_m L_f i \omega + v) \\ \frac{d\omega}{dt} = \frac{1}{J} (K_m L_f i^2 - B \omega - \Gamma_L) \end{cases} \quad (9)$$

Remark 1. Γ_L is considered as a perturbation.

2.1 Per unit model

Model (9) is expressed in SI units. In order to facilitate the comparison of variables, we propose the *per unit* model, whose quantities have no units. Furthermore, all the nominal values become 1, so the absolute value of the new variables are less than 1 most of the time. This per unit system is given by the following scale:

• input :

$$v_{pu} = \frac{v}{V_{nom}} \quad (10)$$

• states :

$$\begin{cases} i_{pu} = \frac{i}{I_{nom}} \\ \omega_{pu} = \frac{\omega}{\omega_{nom}} \end{cases} \quad (11)$$

• perturbation :

$$\Gamma_{Lpu} = \frac{\Gamma_L}{\Gamma_{Lnom}} \quad (12)$$

Then, system (9) becomes:

$$\begin{cases} \frac{di_{pu}}{dt} = \frac{1}{L} \left(-R i_{pu} - K_m L_f \omega_{nom} i_{pu} \omega_{pu} + \frac{V_{nom}}{I_{nom}} v_{pu} \right) \\ \frac{d\omega_{pu}}{dt} = \frac{1}{J} \left(\frac{K_m L_f I_{nom}^2}{\omega_{nom}} i_{pu}^2 - B \omega_{pu} - \frac{\Gamma_{nom}}{\omega_{nom}} \Gamma_{Lpu} \right) \end{cases} \quad (13)$$

3. OBSERVABILITY ANALYSIS OF THE DC SERIES MOTOR

For a reminder of nonlinear observability in the electrical motor context see, for example, Zaitni et al. [2010], section II. In this section we recall the *rank criterion* given by Hermann and Krener [1977]. To do this, we first introduce the *Lie-Bäcklund* derivatives (see Fliess et al. [1999]), noted as:

$$\begin{cases} L_f h = \frac{\partial h}{\partial x} f \\ L_f^2 h = \frac{\partial L_f h}{\partial x} f + \frac{\partial L_f h}{\partial u} \dot{u} \\ L_f^3 h = \frac{\partial^2 L_f h}{\partial x^2} f + \frac{\partial^2 L_f h}{\partial x \partial u} \dot{u} + \frac{\partial L_f^2 h}{\partial \dot{u}} \ddot{u} \\ \vdots \\ L_f^{n-1} h = \frac{\partial L_f^{n-2} h}{\partial x} f + \sum_{i=1}^{n-2} \frac{\partial L_f^{n-2} h}{\partial u^{(i-1)}} u^{(i)} \\ \vdots \\ L_f^p h = \frac{\partial L_f^{p-1} h}{\partial x} f + \sum_{i=1}^{p-1} \frac{\partial L_f^{p-1} h}{\partial u^{(i-1)}} u^{(i)} \end{cases} \quad (14)$$

where $u^{(i)}$ is the i 'th derivation of u , and p is a natural number which may be greater than n .

Criterion 1. (Rank criterion)

Given a system

$$\Sigma : \begin{cases} \dot{x} = f(x) + g(x)u \\ y = h(x) \end{cases} \quad (15)$$

it is *locally regularly weakly observable* at x_0 if:

$$\text{rank}(J_c) = \text{rank} \begin{pmatrix} dh \\ dL_f h \\ dL_f^2 h \\ \vdots \\ dL_f^i h \\ \vdots \\ dL_f^{n-1} h \end{pmatrix} \Big|_{x_0} = n \quad (16)$$

Remark 2. Regularity implies that n derivations of the output (rows of matrix J_c) suffice for the systems Σ to be observable.

Considering the following equivalences, the model of the DC series motor (system (9)) can be written in the form (15):

$$x = \begin{bmatrix} x_1 \\ x_2 \end{bmatrix} = \begin{bmatrix} i \\ \omega \end{bmatrix}, \quad (17)$$

$$u = \begin{bmatrix} u_1 \\ u_2 \end{bmatrix} = \begin{bmatrix} v \\ \Gamma_L \end{bmatrix}, \quad (18)$$

$$f(x) = \begin{bmatrix} f_1(x) \\ f_2(x) \end{bmatrix} = \begin{bmatrix} -\frac{R}{L} x_1 - \frac{K_m L_f}{J} x_1 x_2 \\ \frac{K_m L_f}{J} x_1^2 - \frac{B}{J} x_2 \end{bmatrix}, \quad (19)$$

$$g(x) = \begin{bmatrix} g_1(x) \\ g_2(x) \end{bmatrix} = \begin{bmatrix} 1/L \\ 1/J \end{bmatrix}, \quad (20)$$

$$h(x) = x_1 \quad (21)$$

Remark 3. The output $y = h(x) = x_1$ is the *measured* output (i.e. the current).

We now determine the matrix J_c , given in equation (16). The first row is given by:

$$dh(x) = \begin{bmatrix} \frac{\partial h}{\partial x_1} & \frac{\partial h}{\partial x_2} \end{bmatrix} = [1, 0] \quad (22)$$

To determine the second row we need first to calculate $L_f h$:

$$L_f h = \begin{bmatrix} \frac{\partial h}{\partial x_1} & \frac{\partial h}{\partial x_2} \end{bmatrix} \cdot \begin{bmatrix} f_1(x) \\ f_2(x) \end{bmatrix} = f_1(x) \quad (23)$$

therefore

$$dL_f h = \begin{bmatrix} \frac{\partial f_1(x)}{\partial x_1} & \frac{\partial f_1(x)}{\partial x_2} \end{bmatrix} \quad (24)$$

From (22) and (24) we obtain:

$$J_c = \begin{bmatrix} 1 & 0 \\ \frac{\partial f_1(x)}{\partial x_1} & \frac{\partial f_1(x)}{\partial x_2} \end{bmatrix} \quad (25)$$

The determinant of J_c is:

$$\det(J_c) = \frac{\partial f_1(x)}{\partial x_2} = -\frac{K_m L_f}{L} x_1 \quad (26)$$

which is different from zero *iff* $x_1 \neq 0$. According to the *rank criterion*, the DC series motor is *locally regularly observable* for $x_1 \neq 0$. At zero current, the observability cannot be determined by the rank criterion.

4. OBSERVER DESIGN

In this section we propose a *step-by-step super twisting algorithm* (see Floquet and Barbot [2007] for an overview

of this algorithm) to estimate, in finite time, the speed (ω_{pu}) and the load torque (Γ_{Lpu}). We distinguish two stages in this design: stage 1 and stage 2, where speed and load torque observations are accomplished, respectively.

4.1 Stage 1: speed observation

This stage is associated to the current dynamics (first equation of system (13)). We propose the following change of coordinates to linearize this equation:

$$\begin{cases} z_1 = i_{pu} \\ z_2 = -\frac{K_m L_f \omega_{nom}}{L} i_{pu} \omega_{pu} \\ z_3 = -\frac{\Gamma_{Lnom}}{J \omega_{nom}} \Gamma_{Lpu} \end{cases} \quad (27)$$

So the dynamics of the current (z_1) is as follows:

$$\dot{z}_1 = -\frac{R}{L} z_1 + z_2 + \frac{V_{nom}}{L I_{nom}} v_{pu} \quad (28)$$

which is now linear. We propose the first observation stage:

$$\begin{cases} \dot{\hat{z}}_1 = -\frac{R}{L} z_1 + \tilde{z}_2 + \frac{V_{nom}}{L I_{nom}} v_{pu} + \lambda_1 |e_1|^{1/2} \text{sign}(e_1) \\ \dot{\hat{z}}_2 = \alpha_1 \text{sign}(e_1) \end{cases} \quad (29)$$

where $e_1 = z_1 - \hat{z}_1$, and $\lambda_1, \alpha_1 \in \mathbb{R}$ are tuning parameters. From (28) and (29) we obtain the error dynamics:

$$\begin{cases} \dot{e}_1 = z_2 - \tilde{z}_2 - \lambda_1 |e_1|^{1/2} \text{sign}(e_1) \\ \dot{\tilde{z}}_2 = \alpha_1 \text{sign}(e_1) \end{cases} \quad (30)$$

which is the error dynamics of a *super-twisting* algorithm (see Levant [1998]). If z_2 is a differentiable function with Lipschitz constant C_1 , the following conditions assure that e_1 and \tilde{z}_2 converge, in a finite time T_1 , to zero (see Saadaoui et al. [2006] for a proof of the convergence and an estimation of T_1):

$$\begin{cases} \alpha_1 > C_1 \\ \lambda_1 > \sqrt{\frac{2}{\alpha_1 - C_1}} (\alpha_1 + C_1) \end{cases} \quad (31)$$

Therefore, after a finite time T_1 , \tilde{z}_2 converges to z_2 . Note that the change of coordinates needed to obtain the speed (see next section) presents a singularity at $z_1 = 0$, therefore, the observer cannot be synthesized at zero current.

4.2 Stage 2: load torque observation

This stage is associated to the speed dynamics (second equation of system (13)). A new change of coordinates is proposed:

$$\begin{cases} \chi_1 = z_1 \\ \chi_2 = -\frac{L}{K_m L_f \omega_{nom}} \frac{z_2}{z_1} \quad \text{if } z_1 \neq 0 \\ \chi_3 = z_3 \end{cases} \quad (32)$$

In this coordinate system the speed dynamics is:

$$\dot{\chi}_2 = \frac{K_m L_f I_{nom}^2}{J \omega_{nom}} \chi_1^2 - \frac{B}{J} \chi_2 + \chi_3 \quad (33)$$

We propose the following observer:

$$\begin{cases} \dot{\hat{\chi}}_2 = E_1 \left(\frac{K_m L_f I_{nom}^2}{J \omega_{nom}} \chi_1^2 - \frac{B}{J} \tilde{\chi}_2 + \tilde{\chi}_3 \right. \\ \quad \left. + \lambda_2 |e_2|^{1/2} \text{sign}(e_2) \right) \\ \dot{\hat{\chi}}_3 = E_1 \alpha_2 \text{sign}(e_2) \end{cases} \quad (34)$$

with $e_2 = \chi_2 - \tilde{\chi}_2$, and E_1 defined as follows:

$$\begin{cases} E_1 = 1 & \text{if } |e_1| \leq \varepsilon \\ E_1 = 0 & \text{otherwise} \end{cases} \quad (35)$$

where ε is a sufficiently small positive constant. Once the first stage has converged, $E_1 = 0$ and $\tilde{\chi}_2 \approx \chi_2$. Under these conditions the error dynamics become:

$$\begin{cases} \dot{e}_2 \approx \chi_3 - \tilde{\chi}_3 - \lambda_2 |e_2|^{1/2} \text{sign}(e_2) \\ \dot{\tilde{\chi}}_3 = \alpha_2 \text{sign}(e_2) \end{cases} \quad (36)$$

As in the previous subsection, equation (36) corresponds to the super twisting error dynamics, and $\tilde{\chi}_3$ is proven to converge to χ_3 in a finite time T_2 , for χ_3 differentiable with Lipschitz constant C_2 , under the following conditions:

$$\begin{cases} \alpha_2 > C_2 \\ \lambda_2 > \sqrt{\frac{2}{\alpha_2 - C_2}} (\alpha_2 + C_2) \end{cases} \quad (37)$$

The speed and load torque estimations are given, respectively, by

$$\hat{\omega}_{pu} = \hat{\chi}_2 \quad (38)$$

and

$$\hat{\Gamma}_{Lpu} = -\frac{J \Gamma_{nom}}{\omega_{nom}} \hat{\chi}_3 \quad (39)$$

5. ESTIMATOR

In order to prevent the observer to work near the observability singularity, we suggest the use of the following speed estimator:

$$\dot{\hat{\omega}}_{pu} = -\frac{1}{\tau_{est}} \hat{\omega}_{pu} \quad (40)$$

where τ_{est} is the *mechanical time constant*. This estimator will provide a good speed estimation only in the case where this parameter is well approximated. However, even in the case of bad parameter approximation, this allows us to “simulate” a deceleration in the case of zero current.

5.1 Switching between estimator and observer modes

The switching between estimator and observer modes is given by a condition on the current value. We establish a threshold I_{thr} such that:

- if $|i_{pu}| > I_{thr}$ the speed estimation is done in *observer* mode,
- if $|i_{pu}| \leq I_{thr}$ the speed estimation is done in *estimator* mode.

6. SIMULATION RESULTS

The presented observer/estimator scheme has been simulated in a sensorless speed control context. The motor nominal values and its parameters are shown in table 1. The implemented control is a classical PI, whose parameters are given in table 2. The observer parameters are given in table 3.

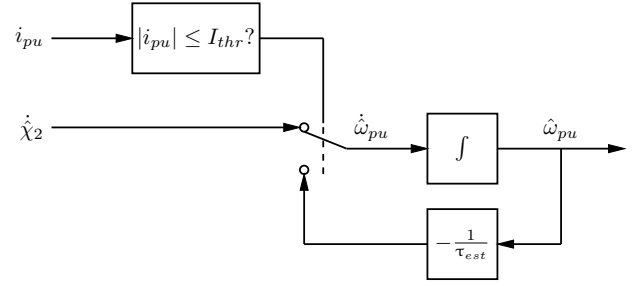


Fig. 1. Switching scheme between observer and estimator modes

Table 1. Motor nominal values and parameters

| Variable | Nominal value |
|----------------|------------------------|
| U_{nom} | 220 V |
| I_{nom} | 15 A |
| ω_{nom} | 104.72 rad/s (1000RPM) |
| Γ_{nom} | 27Nm |
| Parameter | Value |
| R_a | 0.6Ω |
| R_f | 1.8Ω |
| L_a | 1 mH |
| L_f | 220 mH |
| K_m | 0.12 |
| B | 0.02 Nms |
| J | 0.2 Nms ² |

Table 2. PIs parameters

| Parameter | PI speed | PI current |
|-----------|----------|------------|
| k_p | 0.2 | 20 |
| T_i | 0.2 | 0.01 |

Table 3. Observer parameters

| Parameter | Speed stage | Torque stage |
|---------------|-------------|------------------|
| α | 1000 | 7 |
| λ | 70 | 5 |
| ε | – | 10 ⁻⁴ |

6.1 Case 1: loaded motor

This case is presented in figure 2. The observed variables, $\hat{\omega}_{pu}$ and $\hat{\Gamma}_{Lpu}$, converge at about 4 seconds. At this moment, a load torque Γ_L of nominal value is applied. It can be seen that $\hat{\Gamma}_{Lpu}$ exhibits a properly following of this perturbation, and that the overall system performs correctly.

The convergence of the observed speed can be seen in detail in figure 3. At zero seconds, when the observer starts running, $\hat{\omega}_{pu}$ exhibits a “peak” as a consequence of the proximity to the observability singularity (zero current). After that, it presents a negative peak during a few milliseconds. This effects, as well as the chattering (inherent to $\hat{\omega}_{pu}$), are smoothed in the second stage of the observer. The speed observation issued from this stage, i.e. $\hat{\omega}_{pu}$, is then chattering-free and minimizes the destabilizing effects of $\hat{\omega}_{pu}$. This can also be seen in the second zoom, where the load torque is applied.

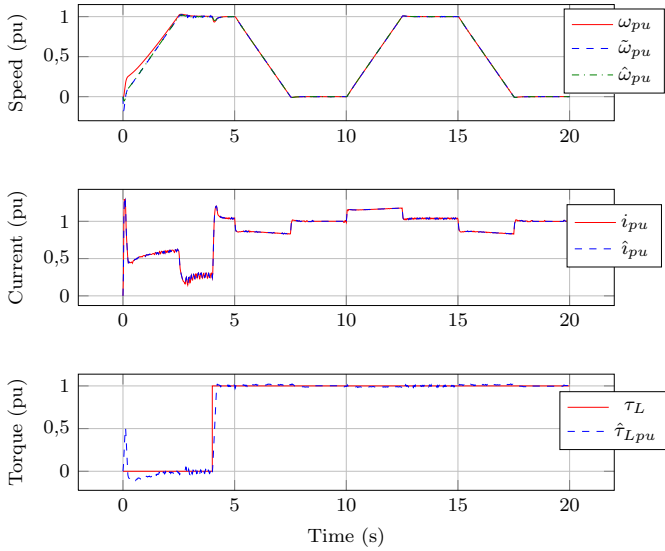


Fig. 2. Simulation results of the sensorless control of the loaded motor

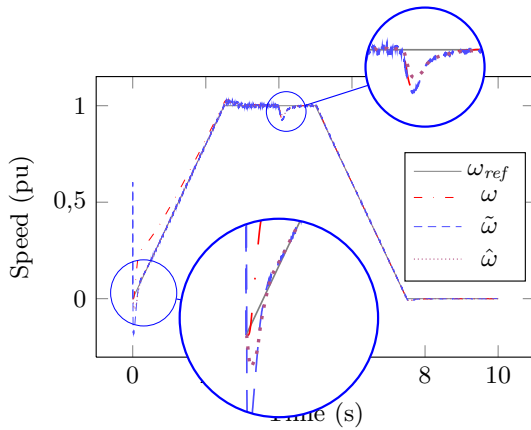


Fig. 3. Sensorless control of the loaded motor. Detail on the speed.

Table 4. Estimator parameters

| Parameter | Value |
|-----------|------------|
| τ | 10s |
| I_{thr} | 0.001 (pu) |

6.2 Case 2: unloaded motor

When no load is coupled to the motor, it is easy to operate at zero or near-zero current. This situation may arrive while decelerating the machine, for example. As we have seen, the speed observer will not work properly (or not at all) under these conditions. An example of such a situation is shown in figure 4, where $\hat{\omega}_{pu}$ takes values higher than 1 when the current is zero. In order to avoid this, an estimator is proposed to complement the observer. Its parameters are presented in table 4. Now, the last simulation is rerun in the presence of the estimator (figure 5). This time, $\hat{\omega}_{pu}$ follows ω_{pu} when the system works near (or in) the observability singularity, while $\tilde{\omega}_{pu}$ diverges. Note that, when $\hat{\omega}_{pu}$ is less than ω_{ref} , the control increases the current to accelerate the motor. This brings the system out from the observability singularity, then the system

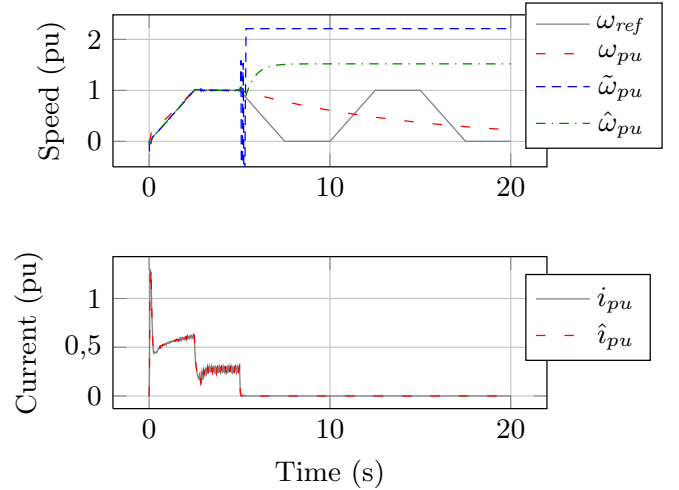


Fig. 4. Sensorless speed control performance at zero current in the absence of estimator

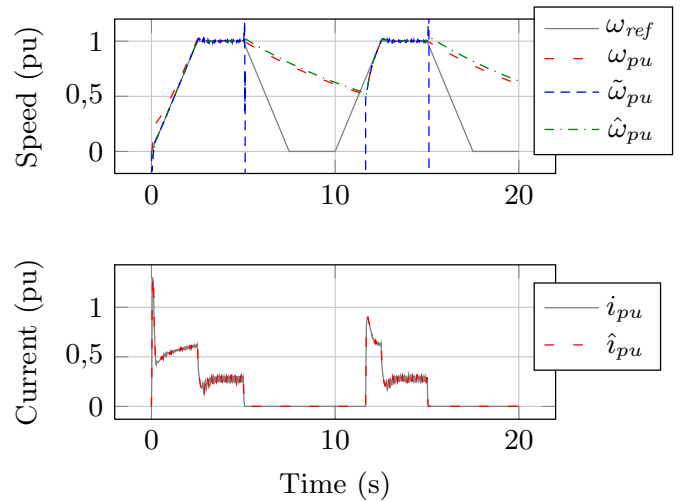


Fig. 5. Sensorless speed control performance at zero current in the presence of estimator

switches to *observer mode*. This causes $\tilde{\omega}_{pu}$ to converge to ω_{ref} , as we can see at about 12 seconds.

Remark 4. τ_{est} was chosen to be equal to the mechanical time constant of the motor (B/J). In practice this parameter may be unknown. In this case, τ_{est} should be chosen to be less than B/J , which allows the estimator to simulate faster decelerations. Otherwise, the control would not be regained when $\omega_{pu} \approx \omega_{ref}$ but when $\hat{\omega}_{pu} \approx \omega_{ref}$, which yields to larger transient currents and accelerations. Both situations have been simulated to illustrate this. In figure 6 the time constant τ_{est} is 5 seconds, while in figure 7 is 20 seconds. Note that in the second case the transient current is much higher when the control is regained.

7. CONCLUSION AND PERSPECTIVES

In this work a sensorless speed control for a DC series motor was presented. An observability analysis revealed an observability singularity at zero current. This led us to design an observer/estimator approach. The proposed observer is based on second order sliding mode techniques, whose excellent properties such as finite time converge,

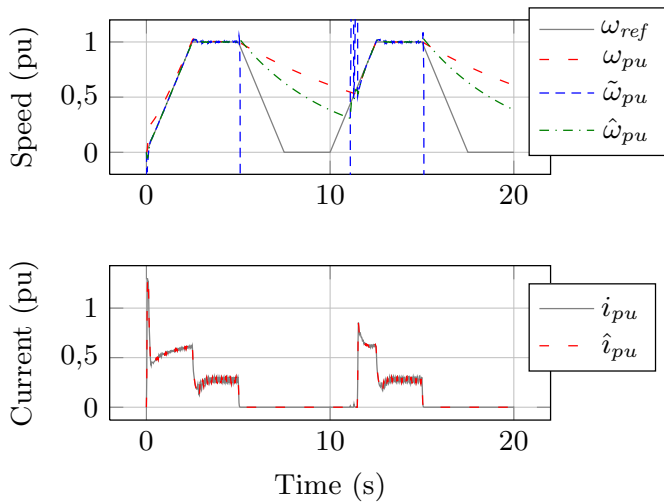


Fig. 6. Sensorless speed control for estimator with $\tau_{est} = 5s$

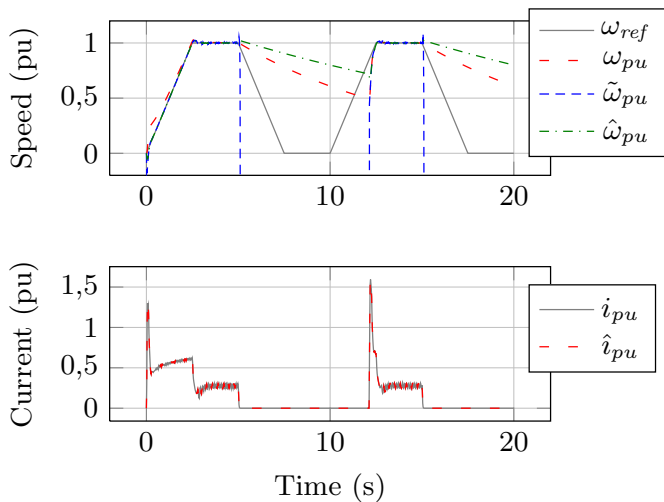


Fig. 7. Sensorless speed control for estimator with $\tau_{est} = 20s$

robustness, and design simplicity with respect to noise are well known. On the other hand, the estimator operates at zero (or near zero) current, providing a speed estimation when it is unobservable. Practical considerations for the estimator design were pointed out, as well. The whole scheme was validated by means of simulations.

Our ongoing work focus on the practical implementation, experimental results, and on the stability proof of the proposed sensorless control.

REFERENCES

M. T. Angulo, J. A. Moreno, and L. Fridman. The differentiation error of noisy signals using the generalized super-twisting differentiator. In *51st IEEE Conference on Decision and Control (CDC)*. IEEE, 2012.

N. Boizot. *Adaptive high-gain extended Kalman filter and applications*. PhD thesis, Université de Bourgogne; Université du Luxembourg, 2010.

N. Boizot, E. Busvelle, J.-P. Gauthier, and J. Sachau. Adaptive gain extended Kalman filter: Application to a series-connected DC motor. In *Conference on Systems and Control*, 2007a.

N. Boizot, E. Busvelle, and J. Sachau. High-gain observers and Kalman filtering in hard real-time. In *RTL 9th Workshop*, 2007b.

M. J. Burrige and Z. Qu. An improved nonlinear control design for series DC motors. *Computers & Electrical Engineering*, 29(2), March 2003. ISSN 00457906.

J. Chiasson. Nonlinear differential-geometric techniques for control of a series DC motor. In *IEEE Transactions on Control Systems Technology*, volume 2, March 1994. doi: 10.1109/87.273108.

Z. Dongbo. An Improved Nonlinear Speed Controller for Series DC Motors. In C. Myung, editor, *IFAC 17th World Congress*, July 2008. ISBN 9781123478.

M. Fliess, J. Lévine, P. Martin, and P. Rouchon. A lie-backlund approach to equivalence and flatness of nonlinear systems. *Automatic Control, IEEE Transactions on*, 44(5), 1999.

T. Floquet and J.P. Barbot. Super twisting algorithm-based step-by-step sliding mode observers for nonlinear systems with unknown inputs. *International Journal of Systems Science*, 38(10), 2007.

R. Hermann and A. Krener. Nonlinear controllability and observability. *IEEE Transactions on Automatic Control*, 22(5), October 1977. ISSN 0018-9286.

D.P. Idracous. Series connected DC motor tracking using port controlled Hamiltonian systems equivalence. In *Proceedings of the 13th WSEAS International Conference on SYSTEMS*, 2009. ISBN 9789604740970.

D.P. Idracous and A.T. Alexandridis. Nonlinear control of a series connected dc motor using singular perturbation and feedback linearization techniques. In *Proceedings of the 3rd European Control conference*, 1995a.

D.P. Idracous and A.T. Alexandridis. Fuzzy tuned PI controllers for series connected DC motor drives. In *Proceedings of the IEEE International Symposium on Industrial Electronics*, volume 2, pages 495–499. IEEE, 1995b. ISBN 0-7803-2683-0.

A. Levant. Robust exact differentiation via sliding mode technique. *Automatica*, 34(3), 1998.

S. Mehta and J. Chiasson. Nonlinear control of a series DC motor: theory and experiment. In *IEEE Transactions on Industrial Electronics*, volume 45, 1998.

H. Saadaoui, N. Manamanni, M. Djemai, J.P. Barbot, and T. Floquet. Exact differentiation and sliding mode observers for switched lagrangian systems. *Nonlinear Analysis: Theory, Methods & Applications*, 65(5), 2006.

J. Santana, J.L. Naredo, F. Sandoval, I. Grout, and O.J. Argueta. Simulation and construction of a speed control for a DC series motor. *Mechatronics*, 12(9-10), November 2002. ISSN 09574158.

I.I. Siller-Alcalá, J. U. Liceaga-Castro, R. Alcántara-Ramírez, and J. Jaimes-Ponce. Speed nonlinear predictive control of a series dc motor for bidirectional operation. In *Proceedings of the 13th IASME/WSEAS*, 2011.

D. Zaltni, M. Ghanes, J.P. Barbot, and M. N. Abdelkrim. Synchronous motor observability study and an improved zero-speed position estimation design. In *49th IEEE Conference on Decision and Control (CDC)*. IEEE, December 2010. ISBN 978-1-4244-7745-6.